



## Get Clarity On Generics

Cost-Effective CT & MRI Contrast Agents



FRESENIUS  
KABI

WATCH VIDEO

# AJNR

This information is current as  
of August 17, 2025.

## **Pixel-by-Pixel Comparison of Volume Transfer Constant and Estimates of Cerebral Blood Volume from Dynamic Contrast-Enhanced and Dynamic Susceptibility Contrast-Enhanced MR Imaging in High-Grade Gliomas**

P. Alcaide-Leon, D. Pareto, E. Martinez-Saez, C. Auger, A.  
Bharatha and A. Rovira

*AJNR Am J Neuroradiol* 2015, 36 (5) 871-876

doi: <https://doi.org/10.3174/ajnr.A4231>

<http://www.ajnr.org/content/36/5/871>

# Pixel-by-Pixel Comparison of Volume Transfer Constant and Estimates of Cerebral Blood Volume from Dynamic Contrast-Enhanced and Dynamic Susceptibility Contrast-Enhanced MR Imaging in High-Grade Gliomas

P. Alcaide-Leon, D. Pareto, E. Martinez-Saez, C. Auger, A. Bharatha, and A. Rovira

## ABSTRACT

**BACKGROUND AND PURPOSE:** Estimates of blood volume and volume transfer constant are parameters commonly used to characterize hemodynamic properties of brain lesions. The purposes of this study were to compare values of volume transfer constant and estimates of blood volume in high-grade gliomas on a pixel-by-pixel basis to comprehend whether they provide different information and to compare estimates of blood volume obtained by dynamic contrast-enhanced MR imaging and dynamic susceptibility contrast-enhanced MR imaging.

**MATERIALS AND METHODS:** Thirty-two patients with biopsy-proved grade IV gliomas underwent dynamic contrast-enhanced MR imaging and dynamic susceptibility contrast-enhanced MR imaging, and parametric maps of volume transfer constant, plasma volume, and CBV maps were calculated. The Spearman rank correlation coefficients among matching values of CBV, volume transfer constant, and plasma volume were calculated on a pixel-by-pixel basis. Comparison of median values of normalized CBV and plasma volume was performed.

**RESULTS:** Weak-but-significant correlation ( $P < .001$ ) was noted for all comparisons. Spearman rank correlation coefficients were as follows: volume transfer constant versus CBV,  $\rho = 0.113$ ; volume transfer constant versus plasma volume,  $\rho = 0.256$ ; CBV versus plasma volume,  $\rho = 0.382$ . We found a statistically significant difference ( $P < .001$ ) for the estimates of blood volume obtained by using dynamic contrast-enhanced MR imaging (mean normalized plasma volume,  $13.89 \pm 11.25$ ) and dynamic susceptibility contrast-enhanced MR imaging (mean normalized CBV,  $4.37 \pm 4.04$ ).

**CONCLUSIONS:** The finding of a very weak correlation between estimates of microvascular density and volume transfer constant suggests that they provide different information. Estimates of blood volume obtained by using dynamic contrast-enhanced MR imaging are significantly higher than those obtained by dynamic susceptibility contrast-enhanced MR imaging in human gliomas, most likely due to the effect of contrast leakage.

**ABBREVIATIONS:** DCE-MR imaging = dynamic contrast-enhanced MR imaging; DSC-MR imaging = dynamic susceptibility contrast-enhanced MR imaging;  $K^{trans}$  = volume transfer constant; Vp = plasma volume;  $\rho$  = Spearman rank correlation coefficient

Characterization of the hemodynamics of glial tumors by MR perfusion is very relevant because tumor aggressiveness and growth are associated with both endothelial hyperplasia and neovascularization.<sup>1</sup>

The 2 most common MR perfusion techniques used in clinical

practice are dynamic susceptibility contrast-enhanced MR imaging (DSC-MR imaging) and dynamic contrast-enhanced MR imaging (DCE-MR imaging).<sup>2</sup> CBV is usually calculated from DSC-MR imaging data, while the volume transfer constant ( $K^{trans}$ ) is usually obtained by using DCE-MR imaging. Both CBV and the volume transfer constant have demonstrated good discriminative power in distinguishing low- and high-grade tumors<sup>3</sup> and utility in predicting prognosis.<sup>4-6</sup>

$K^{trans}$  is defined as the volume transfer constant between plasma and interstitial space. It is often used as a synonym for permeability, but, as defined by Tofts et al,<sup>7</sup> “the measured transfer constant is a potentially intractable combination of flow, permeability, and surface area.” The physiologic significance of  $K^{trans}$  depends on the balance between capillary permeability and blood flow in the tissue of interest. When permeability

Received August 14, 2014; accepted after revision November 9.

From the Department of Radiology, MR Unit (P.A.-L., D.P., C.A., A.R.), and Department of Pathology (E.M.-S.), Hospital Vall d'Hebron, Barcelona, Spain; and Department of Medical Imaging (A.B.), St Michael's Hospital, Toronto, Ontario, Canada.

This work was supported by a grant from the Spanish Society of Radiology (Beca SERAM Industria) in the form of salary for the principal investigator (P.A.-L.).

Please address correspondence to Paula Alcaide-Leon, MD, Hospital Vall d'Hebron, MR Unit, Radiology, Passeig Vall d'Hebron, 119–129, 08035, Barcelona, Spain; e-mail: paulaalcaideleon@hotmail.com

<http://dx.doi.org/10.3174/ajnr.A4231>

is very high, the amount of contrast that leaks out of the vessels depends on the amount of contrast that gets to the capillaries per unit of time. In this situation,  $K^{\text{trans}}$  is equal to the blood plasma flow per unit volume of tissue (Fig 1). In cases of low permeability, the transfer constant equals the permeability surface area product between blood plasma and the extravascular-extracellular space, per unit volume of tissue.

In the brain, most cases are surface area product–limited,<sup>7</sup> so  $K^{\text{trans}}$  depends on both the leakiness of the vessels and the total surface of leaky capillaries. The problem is that the contribution of each factor to the measured  $K^{\text{trans}}$  is a priori unknown. The transfer constant measured in a voxel may be high due to very leaky vessels, a high number of leaky capillaries within the voxel, or a combination of both (Fig 2).

We suggest that within-voxel comparison of blood volume estimates and  $K^{\text{trans}}$  would provide valuable information about physiologic meaning of  $K^{\text{trans}}$  in high-grade gliomas. The correlation between  $K^{\text{trans}}$  and CBV has been previously assessed in gliomas by Law et al.<sup>8</sup> Regions with maximal CBV and maximal  $K^{\text{trans}}$  were compared in each tumor to obtain a weak-but-positive correlation. However, they did not compare parameters of the

same tumor region because their main goal was to correlate maximal values of the parameters with tumor grade. A similar approach was followed by Provenzale et al.<sup>9</sup> They reported a high correlation between CBV and the degree of contrast enhancement, which was defined by the authors as a relative measure of permeability. Again the CBV and  $K^{\text{trans}}$  values used for comparison were obtained from different tumor regions. Results about the correlation between  $K^{\text{trans}}$  and CBV are, therefore, based on indirect methods and are controversial.

The purpose of this study was to compare values of  $K^{\text{trans}}$  and CBV in high-grade gliomas on a pixel-by-pixel basis to determine whether they provide different physiologic information. The second aim was to compare estimates of blood volume obtained by DCE–MR imaging and DSC–MR imaging.

## MATERIALS AND METHODS

### Subjects

We retrospectively reviewed data obtained from 35 consecutive patients with a histopathologic diagnosis of intracranial diffuse astrocytoma with necrosis and/or vascular proliferation (grade IV)<sup>10</sup> who underwent surgery with biopsy or surgical resection at our institution between April 2010 and April 2013 and had pre-operative DSC–MR imaging and DCE–MR imaging data suitable for evaluation obtained in the same setting. None of the patients included in the study had undergone surgery or biopsy of their brain tumor. Some were on steroids, but information about steroid treatment was not always available for this retrospective cohort of patients. Significant displacement of the patient's head between DCE–MR imaging and DSC–MR imaging acquisitions leading to inaccurate coregistration of both sets of images was an exclusion criterion; 3 patients were excluded for this reason (final,  $n = 32$ ). Histopathologic evaluation was performed by 2 experienced neuropathologists and was based on the World Health Organization 2007<sup>10</sup> criteria. Approval was obtained from the ethics committee of Vall d'Hebron Hospital, which waived patient consent for this retrospective study.

### MR Imaging

MR imaging studies were performed on a 3T MR imaging system (Magnetom Trio; Siemens, Erlangen, Germany) by using a 32-

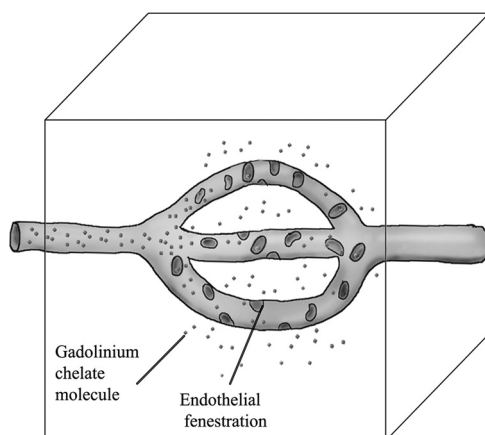


**FIG 1.** Schematic illustrating flow-limited contrast extravasation. Due to high permeability, the rate of leakage within the voxel depends on the amount of plasma reaching the voxel per unit of time (plasma flow). The venous blood would be “clean” of contrast.

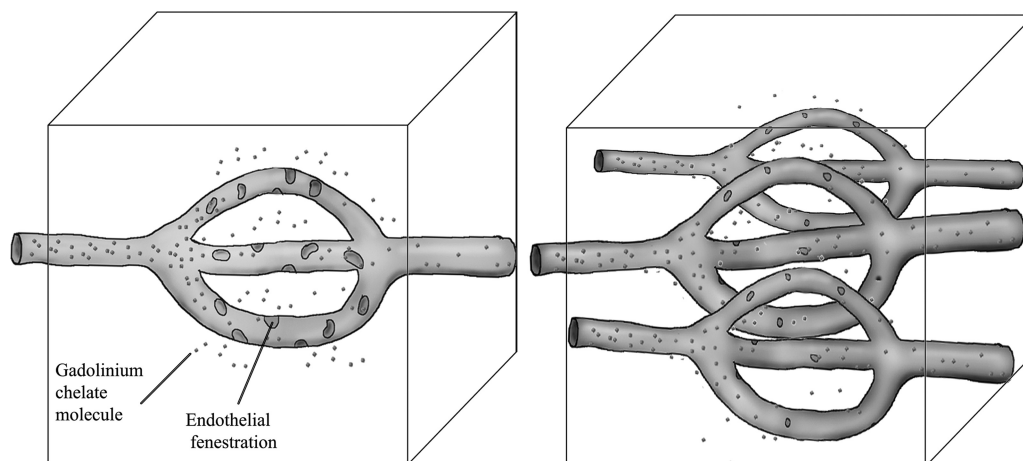


**FIG 2.** Schematic illustrating 2 voxels with similar  $K^{\text{trans}}$  values: the first one showing high permeability and low surface area and the second one with low permeability and high surface area.

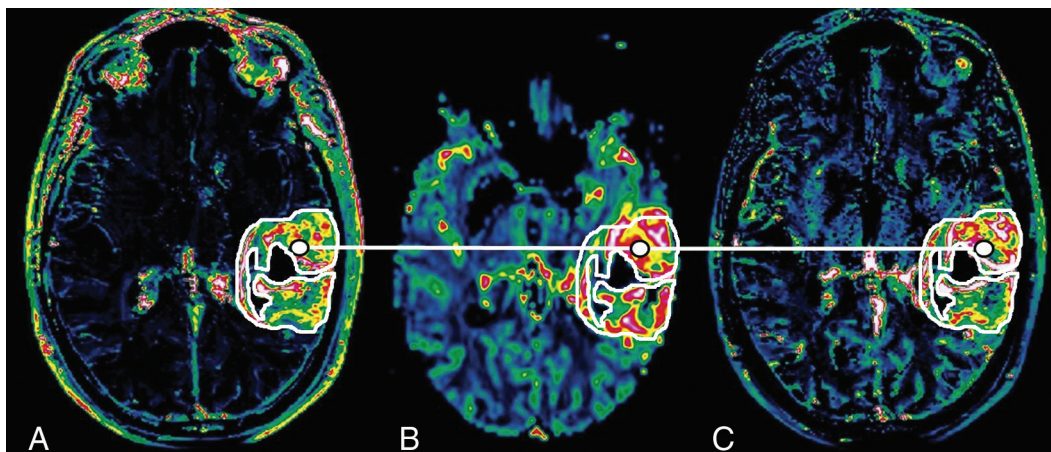


**FIG 3.**  $K^{\text{trans}}$  (A), CBV (B), and Vp (C) maps through the center of a grade IV glioma. The white line connects corresponding pixels for the correlation study.

channel head coil. In a few patients, an 8-channel head coil had to be used instead due to large head size or claustrophobia.

Routine anatomic TSE T2 was performed in all patients before dynamic series (TR/TE, 6100/91 ms; in-plane voxel size,  $0.5 \times 0.4 \times 0.4$  mm; section thickness, 5 mm). Ten sections were selected for DCE-MR imaging to cover the tumor on the basis of T2-weighted images. Sixty consecutive volumes were acquired in 3 minutes 40 seconds (temporal resolution, 6 seconds) by using a T1-weighted sequence (TR/TE, 7.19/2.55 ms; flip angle,  $12^\circ$ ; section thickness, 3.0 mm; matrix,  $320 \times 320$ ; in-plane voxel size,  $1.8 \times 0.7 \times 3.0$  mm). After the first phase was acquired, an intravenous bolus of gadobutrol (Gadovist, 1 mmol/mL; Bayer Schering Pharma, Berlin, Germany) was injected at a dose of 5 mL by using an autoinjector (Spectris Solaris MR injector; MedRad, Indianapolis, Pennsylvania) at a rate of 5 mL/s followed immediately by a 20-mL continuous saline flush injected at a rate of 5 mL/s.

DSC-MR imaging was performed in the transverse plane by using a gradient-echo echo-planar sequence (TR/TE, 1450/45 ms; flip angle,  $90^\circ$ ; FOV, 230 mm; section thickness, 5.0 mm; matrix,  $128 \times 128$ ; in-plane voxel size,  $1.8 \times 1.8 \times 5$  mm). The imaging was performed during the first pass of 5 mL of gadobutrol (Gadovist, 1 mmol/mL), and a series of 60 multisection acquisitions was acquired at 2.9-second intervals during the first pass of contrast agent by using the same autoinjector used for DCE-MR imaging. Administration of contrast material before DSC is known to minimize T1 effects on CBV measurements.<sup>11</sup>

### Image Analysis

DSC and DCE perfusion MR imaging data were transferred to an independent workstation and processed by using the software nordicICE (Version 2.3; NordicNeuroLab, Bergen, Norway). Image processing was performed by 1 of the authors (P.A.-L., with 2 years' experience in neuroradiology). DSC perfusion MR images were used in the production of CBV maps on a voxel-by-voxel basis by use of established tracer kinetic models applied to the first-pass data. To reduce the recirculation effects, the  $\Delta R2^*$  curves were fitted to a  $\gamma$ -variate function, which is an approximation of the first-pass response as it would appear in the absence of recirculation or leakage. The dynamic curves were mathematically corrected to reduce contrast-agent leakage effects.<sup>12</sup> The be-

ginning and the end of the first-pass bolus were determined through inspection of the time-signal intensity curve, and care was taken to exclude any recirculation-related signal intensity. Manual arterial input function detection was used for calculation.

DCE perfusion MR images were used for the steady-state T1 kinetic analysis. This analysis was based on the extended model of Tofts et al,<sup>7</sup> which yields estimates of plasma volume (Vp) and  $K^{\text{trans}}$ . Semiautomated arterial input function detection was used for calculation. The native T1 was not measured, but a fixed value of 1000 ms was assumed. CBV,  $K^{\text{trans}}$ , and Vp maps were automatically coregistered by using nordicICE. This software performs rigid transformation of the datasets by maximization of mutual information.<sup>13</sup>

For each tumor, ROIs were manually drawn on  $K^{\text{trans}}$  maps, including the entire contrast-enhanced region. ROIs were copied to corresponding CBV and Vp maps, and a list of pixel values of the ROIs organized by spatial coordinates was obtained for each map ( $K^{\text{trans}}$ , CBV, and Vp) by using the software package Jim (Version 3.0; Xinapse Systems, West Bergholt, United Kingdom). A 20- to 50-mm<sup>2</sup> ROI was manually drawn on the contralateral normal-appearing white matter for each tumor used to normalize CBV and Vp (normalized CBV = CBV / CBV of normal-appearing white matter; and normalized VP = VP / VP of normal-appearing white matter). Figure 3 illustrates an example of manually drawn ROIs around enhancing tumor in  $K^{\text{trans}}$  (Fig 3A), posteriorly copied to CBV (Fig 3B) and Vp (Fig 3C) maps. Values of pixels in the same tumor location were compared in the correlation study.

Visual inspection of coregistered maps was performed, and 3 patients were excluded from the study because adequate coregistration was impossible to achieve (final,  $n = 32$ ). Sections including susceptibility artifacts due to bone, air, or calcification on CBV maps were excluded. In enhancing tumors, pixels with  $K^{\text{trans}}$  values  $<0.01$  were also excluded from the analysis. This threshold was used to avoid nonenhancing regions that had been previously included in the manually drawn ROIs by mistake. Pixels with normalized CBV and/or Vp  $<0.5$  (half of contralateral normal-appearing white matter) were also excluded because they most likely represented nonenhancing necrotic or edematous areas.



**Table 1: Median, maximum, minimum, and interquartile range of nCBV, nVp, and  $K^{trans}$  values**

	nCBV	nVp	$K^{trans}$ ( $\text{min}^{-1}$ )
Median	3.787	13.2	0.1841
Interquartile range	2.887–5.187	7.806–18.755	0.127–0.3125
Range	1.420–11.271	4.769–62.293	0.0471–0.987

Note:—nCBV indicates normalized CBV; nVp, normalized Vp.

**Table 2: Results of the correlation study performed in a randomly selected sample of 40% (104,171 pixels)**

	CBV and $K^{trans}$	Vp and $K^{trans}$	Vp and CBV
Spearman rank correlation coefficients	0.113 ( $P < .001$ )	0.256 ( $P < .001$ )	0.382 ( $P < .001$ )

### Statistical Analysis

Statistical analysis was performed by using SPSS (IBM, Armonk, New York). Mean values of Vp, CBV, and  $K^{trans}$  of enhancing voxels were calculated for each patient. Values of Vp, CBV, and  $K^{trans}$  were tested for normality and were found to be non-normally distributed. The Kolmogorov-Smirnov test was used for assessing normality. The Spearman  $\rho$  test was used to calculate rank correlation coefficients between corresponding values of  $K^{trans}$  and CBV,  $K^{trans}$  and Vp, and CBV and Vp in each pixel. The Spearman rank correlation coefficient can take values from +1 to -1. A Spearman coefficient of +1 indicates a perfect association. A Spearman coefficient of zero indicates no association between ranks, and a coefficient of -1 indicates a perfect negative association of ranks. The closer the Spearman coefficient is to zero, the weaker the association is between the ranks. Due to large sample size (260,610 pixels), the correlation study was performed for a randomly selected sample of 40%. Comparison between median values of CBV and Vp was made by using the Wilcoxon signed-rank test.

### RESULTS

The mean age of the 32 patients (20 men, 12 women) was 54 years (range, 36–78 years). Total number of enhancing pixels selected was 260,610. The number of pixels selected in each tumor ranged between 489 and 36,385, with an average of 6377.5.

Mean values of normalized CBV, normalized Vp, and  $K^{trans}$  were obtained for each tumor. The distribution of these resulting values was non-Gaussian. Median, maximum, and minimum values and the interquartile ranges of normalized CBV, normalized Vp, and  $K^{trans}$  values are shown in Table 1. The difference between the median values of the normalized estimates of cerebral blood volume and plasma blood volume obtained from DSC-MR imaging and DCE-MR imaging, respectively, was statistically significant ( $P < .001$ ). Results of the correlation study between the parameters CBV,  $K^{trans}$ , and Vp are listed in Table 2.

### DISCUSSION

Values of  $K^{trans}$ , Vp, and CBV obtained in our study have to be interpreted on the basis of all enhancing regions of tumors being included. Most studies in the field of perfusion in human gliomas select small ROIs including maximal CBV values. This difference may explain the presence of low mean CBV compared with those reported in the literature for grade IV tumors.<sup>14</sup>

When we compared Vp and CBV means, a difference between the T1 and T2\* perfusion approaches was evident with blood

volume estimates obtained from DSC-T2 sequences much lower than those obtained from DCE-T1 acquisitions. This difference has been shown by several groups.<sup>15,16</sup> Our results are, therefore, consistent with their hypothesis of blood volume overestimation when the DCE-T1 approach is used and underestimation when the DSC-T2 method is used. This mismatch is thought to be caused by contrast leakage. On DSC-T2, extravascular contrast causes T1 shortening competing with signal drop caused by intravascular contrast. As a result, blood volume is underestimated. In our case, this effect of leakage has been minimized by preloading with contrast before DSC-MR imaging acquisition and performing mathematic corrections to reduce contrast-agent leakage effects. In the case of the DCE-T1 method, extravascular contrast increases the signal of tissue, leading to artificially elevated blood volume values.

We found a very weak positive correlation between Vp and  $K^{trans}$ . Both parameters were obtained from the same sequence, so alignment between both maps was perfect. This low correlation suggests that Vp and  $K^{trans}$  are providing different information.

A very weak positive correlation between CBV and  $K^{trans}$  was found. The correlation was weaker than that between Vp and  $K^{trans}$ , most likely due to the lack of perfect alignment between CBV and  $K^{trans}$  maps. CBV values were obtained from DSC-MR imaging, whereas  $K^{trans}$  and Vp were calculated from the same set of dynamic series. In the case of CBV and  $K^{trans}$ , automated interpolation and coregistration of maps had to be performed before the analysis. Visual inspection revealed coregistration not completely accurate between  $K^{trans}$  and CBV maps, mostly due to spatial distortions resulting from susceptibility effects in the T2\*WI acquisition. Haroon et al<sup>16</sup> reported the same problem when trying to correlate CBV derived from T1 and T2\* sequences in brain tumors.

Correlation between the 2 estimates of microvascular density (CBV and Vp) is also significant and stronger than that between  $K^{trans}$  and CBV and  $K^{trans}$  and Vp. Figure 4 shows an area in the posterior aspect of the tumor showing high CBV and Vp values but not particularly elevated  $K^{trans}$  values. Such a low correlation ( $\rho = 0.382$ ) for 2 parameters, Vp and CBV, which are supposed to provide the same physiologic information (microvessel density), is somewhat surprising. This may be partially explained by slight spatial misregistration as discussed above. Another phenomenon that can account for this low correlation is microscopic hemosiderin deposition, which is known to be present in high-grade gliomas and cause signal loss in T2\* sequences. Although areas of blooming and voxels with very low values were excluded, small effects from microscopic hemosiderin would still be present. Another difference inherent in the techniques that could account for the low correlation is blooming on DSC-MR imaging. The T2\* approach relies on dephasing of the protons within a voxel caused by the intravascular contrast, but the dephasing effect extends to surrounding voxels as well. T1 shortening caused by intravascular contrast on DCE-MR imaging does not extend to surrounding voxels to the same extent.

Few studies correlating  $K^{trans}$  and blood volume in brain tumors have been published, and most take for granted that  $K^{trans}$  represents permeability. Tofts et al<sup>7</sup> argue that in the brain,  $K^{trans}$  depends on both the leakiness of the vessels and the total surface

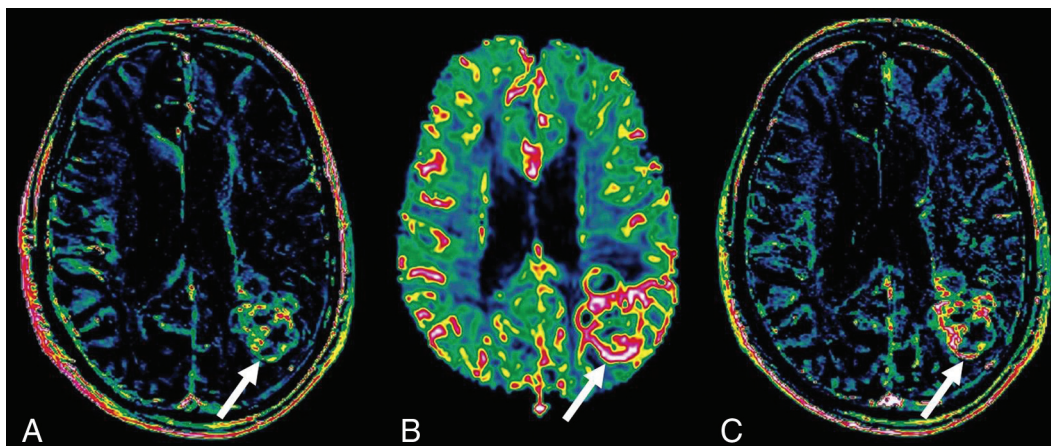


**FIG 4.**  $K^{\text{trans}}$  (A), CBV (B), and Vp (C) maps through the center of a grade IV glioma. The arrow points toward an area in the posterior aspect of the tumor showing high CBV and Vp values but only mildly elevated  $K^{\text{trans}}$  values.

of leaky capillaries, but the contribution of each factor to the  $K^{\text{trans}}$  value is unknown. Estimates of blood volume cannot be used directly as surrogate markers for the surface area of the vessels because it also depends on the diameter of the vessels, which is unknown. Two different tissues may have the same blood volume but different endothelial surface area, depending on the size of the vessels. Thinner but more numerous vessels have higher surface than a smaller number of larger vessels even if the blood volume is the same. Therefore, we cannot reliably conclude that  $K^{\text{trans}}$  is entirely reflecting permeability, but at least we can tell that it is providing different information than estimates of microvessel density.

Correlation studies between  $K^{\text{trans}}$  and CBV have been performed before but never, to our knowledge, on a pixel-by-pixel basis. In a small study including 12 patients with high-grade gliomas, Provenzale et al<sup>9</sup> reported a high correlation between CBV obtained from DSC-MR imaging and maximal enhancement from DCE-MR imaging ( $\rho = 0.794$ ,  $P < .001$ ). They did not assess  $K^{\text{trans}}$  but instead measured an indirect expression of  $K^{\text{trans}}$ , the degree of contrast enhancement using the maximum signal-intensity algorithm. They did not compare parameters from the same tumor region but compared the region with the highest CBV values and the region with the highest “maximal enhancement” values. Patankar et al<sup>3</sup> compared maximal values of CBV and  $K^{\text{trans}}$  obtained from a DCE-MR imaging study in 39 patients and found a high correlation ( $\rho = 0.688$ ,  $P < .001$ ). In a larger study including 73 subjects, Law et al<sup>8</sup> found a weak-but-positive correlation between  $K^{\text{trans}}$  and CBV with a  $\rho$  of 0.266. In this case, both parameters were obtained from the same DSC sequence by using a first-pass pharmacokinetic model. Again parameters were not extracted from the same tumor region. They actually pointed out that the regions of maximal CBV elevation did not directly correspond to the regions of maximal  $K^{\text{trans}}$ . In our study  $K^{\text{trans}}$ , Vp, and CBV values used for comparison were extracted from the same tumor areas.

Our results provide important information regarding imaging biomarkers of angiogenesis in high-grade gliomas. A deep understanding of the physiologic significance of the parameters obtained with DCE and DSC perfusion is very important because both techniques are used in the assessment of antiangiogenic ther-

apies<sup>17,18</sup> and in the differentiation between posttreatment changes and recurrent tumor.<sup>19–22</sup> The assessment of the blood-brain barrier has also gained importance because it provides valuable information regarding brain drug penetration. New therapies have emerged, such as focused sonography, that cause a temporary increase of blood-brain barrier permeability to maximize the delivery of chemotherapy within the brain tumor.<sup>23</sup> Our results confirm that  $K^{\text{trans}}$  and CBV provide very different information, suggesting that it would be worthwhile to perform both DSC- and DCE-MR imaging studies in the setting of gliomas on a routine basis.

One of the main limitations of this study is the lack of T1 mapping for the calculation of contrast concentration in tissue. Our protocol did not include precontrast T1 sequences for T1 mapping calculation, so a fixed baseline T1 value had to be used for  $K^{\text{trans}}$  calculation. Some studies have shown  $K^{\text{trans}}$  estimates to vary on the basis of native T1 values<sup>24</sup>; however, others have used assumptions similar to those used in this study (fixed T1 value), assuming that this is a minor limitation.<sup>25</sup> Another limitation is the inaccurate alignment of maps obtained from DCE-MR imaging (Vp and  $K^{\text{trans}}$ ) and DSC-MR imaging (CBV). This misalignment problem leads to an artifactual decrease in the correlation between CBV and  $K^{\text{trans}}$  values and between CBV and Vp. Misregistration may be causing a decrease in the values of the correlation coefficients but not in all cases because Vp and  $K^{\text{trans}}$  maps are obtained from the same sequence, so alignment is perfect between these maps. A fact that is proving the reliability of the results is that the correlation between CBV and Vp is higher than that between  $K^{\text{trans}}$  and the estimates of microvessel attenuation (CBV and Vp), even though CBV and Vp are obtained from different sequences and therefore subject to misregistration. The correlation between CBV and Vp is higher as expected because both parameters have the same physiologic meaning. The temporal resolution used in our DSC-MR imaging studies (2.9 seconds) is lower than the recommended  $<1.5$  seconds.<sup>26</sup> This difference may cause a decrease in the accuracy of the CBV estimation.

## CONCLUSIONS

The finding of only weak correlation between estimates of blood volume (Vp and CBV) and  $K^{\text{trans}}$  suggests that they provide dif-

ferent physiologic information and that a protocol combining DCE- and DSC-MR imaging may provide complementary information in the imaging work-up of high-grade tumors. Estimates of microvascular attenuation derived from DCE-MR imaging tend to be higher than values of CBV obtained by using DSC-MR imaging, most likely due to overestimation caused by leakage.

Disclosures: Paula Alcaide-Leon—RELATED: Grant: Beca “SERAM Industria” de la Sociedad Española de Radiología Médica; UNRELATED: Employment: Novartis,\* Comments: currently a Research Fellow in multiple sclerosis at St Michael’s Hospital. This fellowship is funded by Novartis. Alex Rovira—UNRELATED: Consultancy: Novartis, Bayer, Biogen; Payment for Lectures (including service on Speakers Bureaus): Novartis,\* Bayer,\* Genzyme,\* Bracco,\* Biogen,\* Stendhal\*; Payment for Development of Educational Presentations: Novartis,\* MS Forum. \*Money paid to the institution.

## REFERENCES

1. Burger PC. Malignant astrocytic neoplasms: classification, pathologic anatomy, and response to treatment. *Semin Oncol* 1986;13:16–26
2. Lüdemann L, Warmuth C, Plotkin M, et al. Brain tumor perfusion: comparison of dynamic contrast enhanced magnetic resonance imaging using T1, T2, and T2\* contrast, pulsed arterial spin labeling, and H2(15)O positron emission tomography. *Eur J Radiol* 2009;70:465–74
3. Patankar TF, Haroon HA, Mills SJ, et al. Is volume transfer coefficient (Ktrans) related to histologic grade in human gliomas? *AJNR Am J Neuroradiol* 2005;26:2455–65
4. Mills SJ, Patankar TA, Haroon HA, et al. Do cerebral blood volume and contrast transfer coefficient predict prognosis in human glioma? *AJNR Am J Neuroradiol* 2006;27:853–58
5. Bisdas S, Kirkpatrick M, Giglio P, et al. Cerebral blood volume measurements by perfusion-weighted MR imaging in gliomas: ready for prime time in predicting short-term outcome and recurrent disease? *AJNR Am J Neuroradiol* 2009;30:681–88
6. Cao Y, Tsien CI, Nagesh V, et al. Survival prediction in high-grade gliomas by MRI perfusion before and during early stage of RT [corrected]. *Int J Radiat Oncol Biol Phys* 2006;64:876–85
7. Tofts PS, Brix G, Buckley DL, et al. Estimating kinetic parameters from dynamic contrast-enhanced T(1)-weighted MRI of a diffusible tracer: standardized quantities and symbols. *J Magn Reson Imaging* 1999;10:223–32
8. Law M, Yang S, Babb JS, et al. Comparison of cerebral blood volume and vascular permeability from dynamic susceptibility contrast-enhanced perfusion MR imaging with glioma grade. *AJNR Am J Neuroradiol* 2004;25:746–55
9. Provenzale JM, York G, Moya MG, et al. Correlation of relative permeability and relative cerebral blood volume in high-grade cerebral neoplasms. *AJR Am J Roentgenol* 2006;187:1036–42
10. Louis DN, Ohgaki H, Wiestler OD, et al. The 2007 WHO classification of tumours of the central nervous system. *Acta Neuropathol* 2007;114:97–109
11. Paulson ES, Schmainda KM. Comparison of dynamic susceptibility-weighted contrast-enhanced MR methods: recommendations for measuring relative cerebral blood volume in brain tumors. *Radiology* 2008;249:601–13
12. Boxerman JL, Schmainda KM, Weisskoff RM. Relative cerebral blood volume maps corrected for contrast agent extravasation significantly correlate with glioma tumor grade, whereas uncorrected maps do not. *AJNR Am J Neuroradiol* 2006;27:859–67
13. Wells WM 3rd, Viola P, Atsumi H, et al. Multi-modal volume registration by maximization of mutual information. *Med Image Anal* 1996;1:35–51
14. Aronen HJ, Gazit IE, Louis DN, et al. Cerebral blood volume maps of gliomas: comparison with tumor grade and histologic findings. *Radiology* 1994;191:41–51
15. Bruening R, Kwong KK, Vevea MJ, et al. Echo-planar MR determination of relative cerebral blood volume in human brain tumors: T1 versus T2 weighting. *AJNR Am J Neuroradiol* 1996;17:831–40
16. Haroon HA, Patankar TF, Zhu XP, et al. Comparison of cerebral blood volume maps generated from T2\* and T1 weighted MRI data in intra-axial cerebral tumours. *Br J Radiol* 2007;80:161–68
17. Jalali S, Chung C, Foltz W, et al. MRI biomarkers identify the differential response of glioblastoma multiforme to anti-angiogenic therapy. *Neuro Oncol* 2014;16:868–79
18. Sorensen AG, Batchelor TT, Zhang WT, et al. A “vascular normalization index” as potential mechanistic biomarker to predict survival after a single dose of cediranib in recurrent glioblastoma patients. *Cancer Res* 2009;69:5296–300
19. Fatterpekar GM, Galheigo D, Narayana A, et al. Treatment-related change versus tumor recurrence in high-grade gliomas: a diagnostic conundrum—use of dynamic susceptibility contrast-enhanced (DSC) perfusion MRI. *AJR Am J Roentgenol* 2012;198:19–26
20. Shin KE, Ahn KJ, Choi HS, et al. DCE and DSC MR perfusion imaging in the differentiation of recurrent tumour from treatment-related changes in patients with glioma. *Clin Radiol* 2014;69:e264–72
21. Sugahara T, Korogi Y, Tomiguchi S, et al. Post-therapeutic intra-axial brain tumor: the value of perfusion-sensitive contrast-enhanced MR imaging for differentiating tumor recurrence from nonneoplastic contrast-enhancing tissue. *AJNR Am J Neuroradiol* 2000;21:901–09
22. Mangla R, Singh G, Ziegelitz D, et al. Changes in relative cerebral blood volume 1 month after radiation-temozolomide therapy can help predict overall survival in patients with glioblastoma. *Radiology* 2010;256:575–84
23. Yang FY, Ko CE, Huang SY, et al. Pharmacokinetic changes induced by focused ultrasound in glioma-bearing rats as measured by dynamic contrast-enhanced MRI. *PLoS One* 2014;9:e92910
24. Guo JY, Reddick WE, Rosen MA, et al. Dynamic contrast-enhanced magnetic resonance imaging parameters independent of baseline T10 values. *Magn Reson Imaging* 2009;27:1208–15
25. Jung SC, Yeom JA, Kim JH, et al. Glioma: application of histogram analysis of pharmacokinetic parameters from T1-weighted dynamic contrast-enhanced MR imaging to tumor grading. *AJNR Am J Neuroradiol* 2014;35:1103–10
26. Essig M, Shiroishi MS, Nguyen TB, et al. Perfusion MRI: the five most frequently asked technical questions. *AJR Am J Roentgenol* 2013;200:24–34